Nucleic Acids Research Advance Access published November 5, 2008

Nucleic Acids Research, 2008, 1–9
doi:10.1093/nar/gkn836

Reinitiated viral RNA-dependent RNA polymerase resumes replication at a reduced rate

Igor D. Vilfan[1], Andrea Candelli[1], Susanne Hage[1], Antti P. Aalto[2], Minna M. Poranen[2], Dennis H. Bamford[2] and Nynke H. Dekker[1,*]

[1]Kavli Institute of Nanoscience, Faculty of Applied Sciences, Delft University of Technology, Lorentzweg 1, 2628 CJ Delft, The Netherlands and [2]Institute of Biotechnology and Department of Biological and Environmental Sciences, Viikki Biocenter, P.O. Box 56, 00014 University of Helsinki, Finland

Received August 27, 2008; Revised and Accepted October 14, 2008

ABSTRACT

RNA-dependent RNA polymerases (*RdRP*) form an important class of enzymes that is responsible for genome replication and transcription in RNA viruses and involved in the regulation of RNA interference in plants and fungi. The *RdRP* kinetics have been extensively studied, but pausing, an important regulatory mechanism for RNA polymerases that has also been implicated in RNA recombination, has not been considered. Here, we report that *RdRP* experience a dramatic, long-lived decrease in its elongation rate when it is reinitiated following stalling. The rate decrease has an intriguingly weak temperature dependence, is independent of both the nucleotide concentration during stalling and the length of the RNA transcribed prior to stalling; however it is sensitive to RNA structure. This allows us to delineate the potential factors underlying this irreversible conversion of the elongation complex to a less active mode.

INTRODUCTION

Template-directed polymerization of nucleotides (NTPs) is an essential process in all living entities. Accordingly, enzymes catalyzing these processes operate in both cellular organisms and in viruses. In RNA viruses, RNA-dependent RNA polymerases (*RdRP*s) are the essential catalytic components of the polymerization machinery. *RdRP*s are also encoded by numerous cellular organisms, where they initiate or amplify the regulatory mechanisms known as RNA silencing (1). The structure and reaction mechanisms of viral *RdRP*s display similarity with many other nucleic acid polymerases, but nonetheless incorporate subtle differences. For instance, viral *RdRP*s adopt the 'right hand-like' conformation typical for numerous nucleic acid polymerases, but they display a distinct 'closed-hand' conformation, rather than the more common 'open-hand' structure (2,3).

Viral *RdRP*s are capable of carrying out two distinct reactions, replication and transcription. These reactions are completed in four steps: (i) template recognition and binding, (ii) initiation, (iii) elongation and (iv) termination. The binding of viral *RdRP*s to template RNA exhibits characteristically low binding constants (4,5), but binding may nonetheless be enhanced by specific nucleotide sequences and/or RNA secondary structures (6,7). During initiation and elongation, viral RdRPs perform a nucleotidyl transfer reaction to polymerize the complementary RNA strand (8). While RNA or protein primers may be required for initiation, most *RdRP*s initiate RNA synthesis *de novo* (3).

To date, the kinetic studies of viral *RdRP* mechanism have neglected the effect of viral *RdRP* stalling. Partial RNA products isolated from poliovirus- and tobacco mosaic virus-infected cells suggest that the *RdRP* indeed frequently stalls, leading to compromised processivity during RNA elongation *in vivo* (9). It has been suggested that viral *RdRP* pausing could be brought about by specific RNA sequences and secondary structures (9), and is likely a prerequisite for viral RNA recombination (10,11). Furthermore, rational drug design against viral *RdRP*s could benefit from the analysis of stalled viral *RdRP*s (12). Finally, while stalling of viral *RdRP*s has been utilized to separate the elongation and initiation stages of the replication and transcription reactions (13), the consequences of stalling on the elongation rates have not been examined.

To quantitatively study the effect of stalling on the kinetics of viral *RdRP*s, we have used the *RdRP* from bacteriophage $\phi 6$ ($\phi 6$ *RdRP*) as a model system (Figure 1A). $\phi 6$ *RdRP* catalyzes primer-independent *de novo* RNA synthesis on single-stranded RNA (ssRNA) and double-stranded RNA (dsRNA) templates and

*To whom the correspondence should be addressed. Tel: +31 (0)15 278 3219; Fax: +31 (0)15 278 1202; Email: n.h.dekker@tudelft.nl
Present address:
Andrea Candelli, Department of Physics and Astronomy, Vrije Universiteit, 1081 HV Amsterdam, The Netherlands

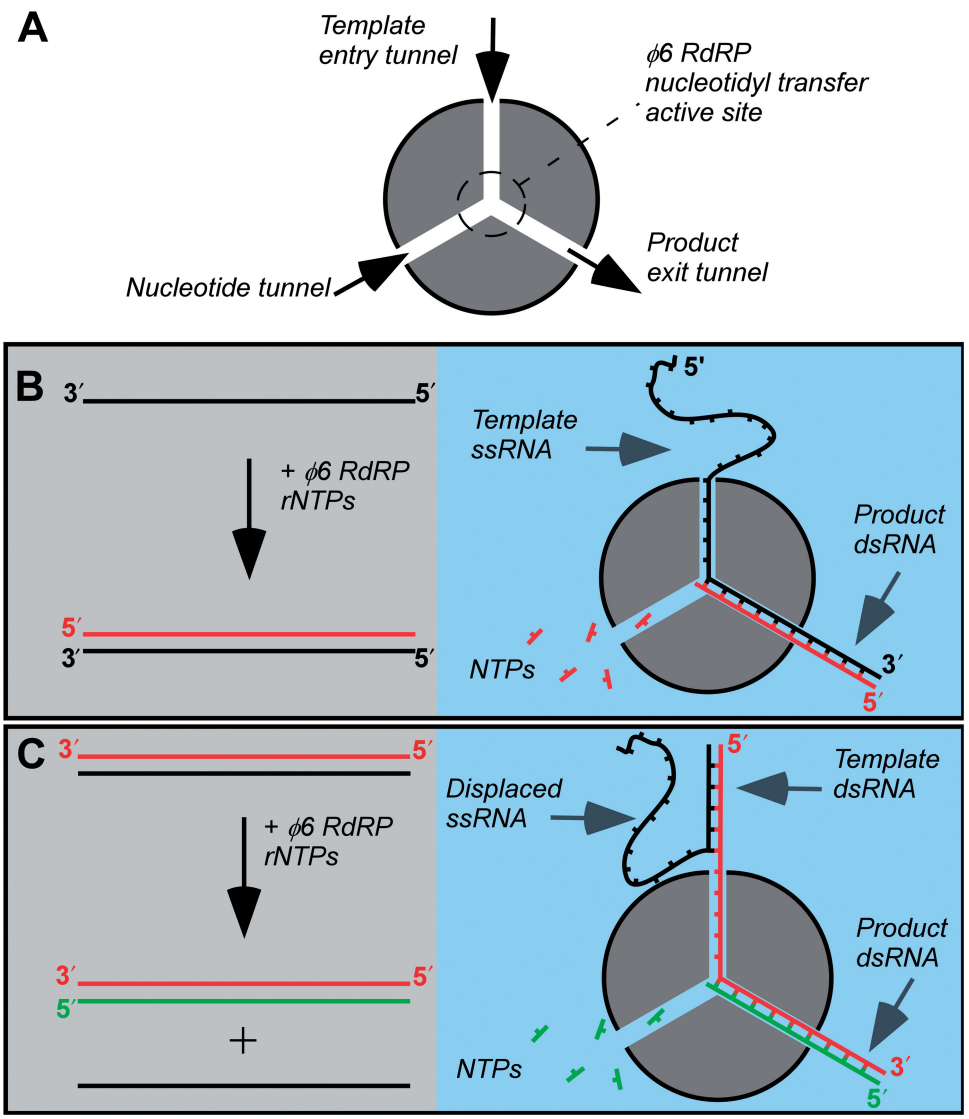

Figure 1. Bacteriophage *ϕ6 RdRP* performs replication and transcription. **(A)** A schematic of the *ϕ6 RdRP* structure. A nucleotidyl transfer active site is linked to the enzyme surface via three tunnels: the template entry tunnel, the NTP tunnel, and the product exit tunnel. **(B)** During replication, a complementary antisense RNA strand [(−)RNA; red line] is polymerized onto a sense RNA template [(+)RNA; black line]. The 3′-end of the template strand accesses the enzyme's active site through the template tunnel. In the presence of NTPs, product dsRNA exits through the product tunnel. **(C)** During transcription, the (+)RNA strand is displaced while *ϕ6 RdRP* polymerizes a new (+)RNA strand (green line) onto the (−)RNA template. Here, the dsRNA genome is first unwound, and the (+)RNA strand is displaced at the entrance to the template tunnel, allowing only the (−)RNA strand to enter the template tunnel. The dsRNA product exits through the product tunnel. The polarities of the RNA strands are indicated in the schematics.

elongates with high processivity (14). During replication, the single-stranded sense RNA strand [(+)RNA] serves as the template for conversion to a dsRNA genome (Figure 1B). In contrast, during transcription, the (−)RNA strand within the dsRNA genome serves as the template for a new (+)RNA strand, which leaves the original (+)RNA strand as a single-stranded by-product (Figure 1C). In both processes, *ϕ6 RdRP* initiates exclusively at the free 3′-end of the template strand, which enters the *ϕ6 RdRP* through the template tunnel leading from the polymerase surface to the active site in the center of the enzyme structure (Figure 1A). By contrast, internal initiation of the elongation complex is not thought to occur (Supplementary Figure S1) (15).

Here, we measure the rate of RNA elongation by *ϕ6 RdRP* and demonstrate that while it is possible to reinitiate the polymerase following stalling induced by nucleotide deprivation, the resulting elongation rate is drastically and irreversibly reduced. This was quantified by measuring the elongation rate of the reinitiated complex using gel electrophoresis. Neither the NTP concentration nor the length of the RNA synthesized prior to stalling had an effect on the rate reduction following reinitiation. We attribute the reduction in the elongation rate to a transition to a sub-optimal conformational state of the elongation complex, brought about by stalling, and demonstrate that the conversion to the sub-optimal conformational state depends on the structure of the RNA

template. In addition to the potential biological importance of the stalling, *in vitro* studies of polymerases have used stalling to measure elongation rates (13,16–18). In light of our findings, it is important to design the experimental setup in a way that a possible reduction in the elongation rate due to stalling is taken into account.

MATERIALS AND METHODS

Purification of the recombinant *RdRP* from bacteriophage *ϕ6*

The *NdeI–EcoRI* restriction fragment from pEM2 plasmid (14) was transferred into a pET-28a(+) vector (Novagen, USA). The resultant plasmid pAA5 was propagated in *Escherichia coli* BL21(DE3) (19). *ϕ6 RdRP* was expressed as previously described (14), except for 25 μg/ml kanamycin. The cells were harvested and resuspended in 50 mM Tris–HCl (pH 8.0), 300 mM NaCl, 1 mM imidazole and disrupted. The supernatant was loaded onto a Ni-NTA affinity column (Qiagen, Valencia, CA, USA). After two successive washes with imidazole buffers (10 mM and 20 mM), *ϕ6 RdRP* was eluted in 50 mM Tris–HCl (pH 8.0), 300 mM NaCl, 250 mM imidazole. Further purification was done using HiTrap™ Heparin HP and Q HP columns (GE Healthcare, USA). *ϕ6 RdRP* was eluted with a linear NaCl gradient (from 0.1 M–1 M NaCl) in 50 mM Tris–HCl (pH 8.0), 0.1 mM EDTA. The purified protein was stored in the elution buffer (containing 300 mM NaCl) at 4°C.

Preparation of RNA molecules

ssRNAs were obtained via *in vitro* run-off transcription using PCR-amplified sections of the pBB10 plasmid (20) as described previously (primers listed in Table S1) (21). To favor terminal incorporation of cytidine into the 3′-end of the transcripts used as templates for *ϕ6 RdRP*, the transcription mixtures were supplemented with 20 mM CTP.

dsRNA molecules were obtained by hybridizing complementary ssRNAs in 0.5 × SSC (Promega, Madison, WI, USA) using a 'gradual-cool' temperature program (21). dsRNA template for transcription reactions was obtained by hybridizing three RNA molecules (4 kb RNA, 1.3 kb RNA and 4 kb 'main' RNA) in a molar ratio of 1:1:1. Alternatively, a molar ratio of 1:4 was used in hybridizations between longer and shorter complementary ssRNA molecules for calibration of the electrophoretic mobilities. All hybridized RNAs were purified as described in (21).

A kinetic study of elongation by reinitiation of stalled *ϕ6 RdRP*

The elongation rate of *ϕ6 RdRP* was typically assayed in a reaction mixture containing 80 nM RNA template, 2.6 μM *ϕ6 RdRP*, 50 mM HEPES pH 7.9, 20 mM ammonium acetate, 5 mM $MgCl_2$, 2 mM $MnCl_2$, 0.1 mM EDTA pH 8.0, 0.1% Triton X-100, 5% (v/v) Superase•In, and 2.5 mM of each nucleotide. A 10-fold lower enzyme to RNA template ratio was tested and shown to have no effect on the kinetics of the reinitiated reaction (data not shown). Prior to the reactions, RNA was heat-denatured by incubation at 65°C for 15 min, followed by fast cooling to 4°C. The 'stalled' reactions were initiated using only three NTPs (ATP, CTP, and GTP). The 'unstalled' reactions were incubated in the absence of NTPs for the same time period. After 15 min incubation at temperature T_1, the temperatures of the stalled and unstalled reactions were changed to temperature T_2, and left to equilibrate for 5 min. The stalled *ϕ6EC*s were reinitiated by adding UTP, and the unstalled reactions were initiated by the addition of all four NTPs. Aliquots were taken at different time points after the addition of missing nucleotides, mixed with EDTA to 45 mM final concentration, and placed on ice. The products were analyzed using 0.75% or 1.5% agarose gels for the transcription and replication reactions, respectively. The agarose gels were preloaded at 2 V/cm for 15 min, and the electrophoresis was carried out at 5 V/cm at 4°C. The reaction products were visualized with ethidium bromide staining. The electrophoretic mobilities of the RNA replication intermediates were compared to a 2-log DNA ladder calibrated using a series of RNA hybrids (Supplementary Data and Figure S2). For experiments including a heparin trap (13), 9 mg/ml heparin (Sigma-Aldrich, St. Louis, MO, USA) was added after the stalling reactions, and the reactions were incubated at 22°C for 5 min prior to the addition of UTP.

RESULTS

Reinitiated *ϕ6EC* replicates with a reduced rate

In replication, a *ϕ6 RdRP* elongation complex (*ϕ6EC*) can be stalled *in vitro* using a limited selection of NTPs and a template molecule in which the 3′-terminal region is devoid of one or more of the nucleotides (Figure 2A; for proof of stalling on short oligos, see Supplementary Data and Figure S3). Elongation can then be reinitiated by the addition of the missing NTP(s), yielding an entirely double-stranded product. To study the effect of stalling on the rate of *ϕ6 RdRP* replication, we selected a 4193 nt long replication template (4 kb ssRNA) in which the first occurrence of adenine was 50 nt from the 3′-end. The stalled *ϕ6EC* exhibited an electrophoretic mobility indistinguishable from that of free 4 kb ssRNA (Supplementary Figure S4). Following stalling and reinitiation by UTP addition, aliquots were collected at successive time points and analyzed on agarose gel (Figure 2B). After reinitiation, a fraction of the replication template retained the electrophoretic mobility of free 4 kb ssRNA (Supplementary Figure 2B, lanes 2–10), which corresponds to either free 4 kb ssRNA or to inactive stalled *ϕ6EC*. The electrophoretic mobility of successfully reinitiated *ϕ6ECs* decreased with time as *ϕ6 RdRP* progressed along the 4 kb ssRNA (Figure 2B, lanes 2–10). Notably, the band corresponding to the reinitiated *ϕ6EC*s stayed well-defined, suggesting that the stalled *ϕ6EC*s reinitiated in a synchronized manner. Termination of the replication reaction was detected by a stabilization of the electrophoretic mobility of the reinitiated *ϕ6ECs* (data not shown). This occurred between 30 min and 60 min after reinitiation, from which

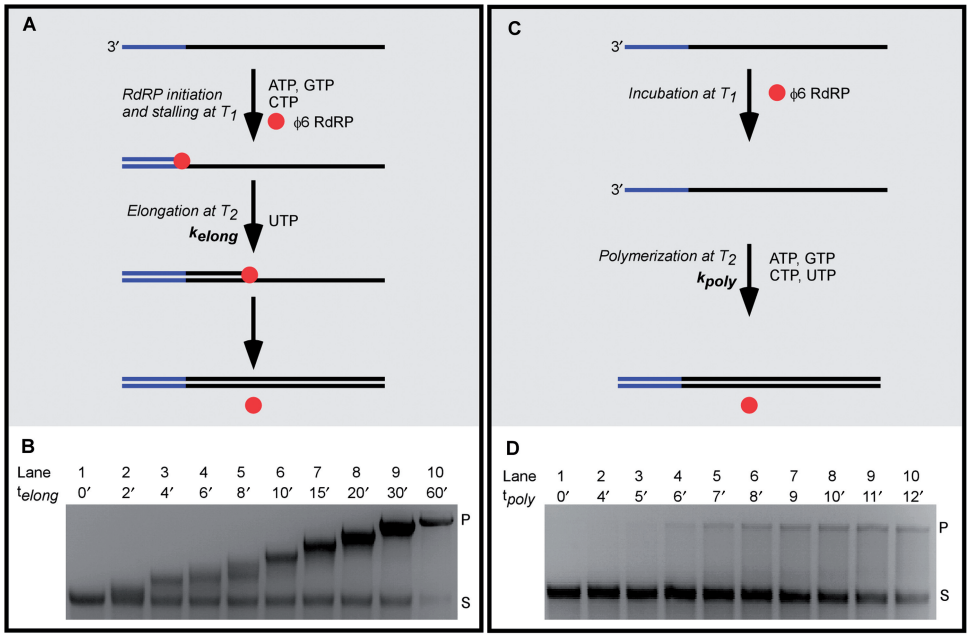

Figure 2. A reinitiated *ϕ6 RdRP* elongation complex (*ϕ6EC*) and randomly-initiated *ϕ6 RdRP* replication show distinct electrophoretic profiles on agarose gels. **(A)** Schematic of stalling and reinitiation of *ϕ6EC*. In the presence of three NTPs (ATP, GTP, CTP), a *ϕ6EC* is stalled at the 50th nt from the 3′-end of the template at temperature T_1. The sequence elongated prior to stalling is shown in blue. After UTP addition, the stalled *ϕ6EC* reinitiates and synthesizes the complementary strand at temperature T_2. **(B)** Agarose gel of the elongation intermediates after reinitiation of the stalled *ϕ6EC* on 4 kb ssRNA template. Aliquots were taken at different times after reinitiation (t_{elong}). Letters S and P indicate 4 kb ssRNA and 4 kb dsRNA, respectively. **(C)** Schematic of a randomly-initiated *ϕ6 RdRP* replication. 4 kb ssRNA was incubated with *ϕ6 RdRP*, and all four NTPs were subsequently added simultaneously. **(D)** Agarose gel of aliquots of randomly-initiated *ϕ6 RdRP* replication taken at different polymerization times (t_{poly}).

we deduce an overall k_{elong} between 1.2 and 2.3 nt·s^{-1}. (For the discussion of the measured rates please see Supplementary Data).

A control experiment was carried out to measure the overall replication polymerization rate (k_{poly}) of unstalled *ϕ6 RdRP* under identical reaction conditions (Figure 2C). To measure k_{poly}, the 4 kb ssRNA was first incubated with *ϕ6 RdRP* for the same duration as above, but in the absence of NTPs. Subsequently, all four NTPs were simultaneously added and aliquots were taken at successive time points. At time zero, only free 4 kb ssRNA could be detected (Figure 2C, lane 1). In contrast to the reinitiated *ϕ6EC*s, at later times distinct bands could *only* be detected for the free 4 kb ssRNA and the final replication product (4 kb dsRNA) (Figure 2C, lanes 2–10), consistent with an unsynchronized population of *ϕ6EC*s in this experiment. The first appearance of 4 kb dsRNA product occurred 6 min after the addition of NTPs (Figure 2C, Lane 4), corresponding to a minimal k_{poly} of 12 nt s^{-1}. Surprisingly, the observed k_{poly} is at least six-fold higher than k_{elong}, despite the fact that k_{poly} is a composite of k_{elong} and the rates of accompanying initial stages of replication (e.g. *ϕ6 RdRP* binding and initiation of *ϕ6EC*). This suggests that the randomly-initiated *ϕ6EC* elongates considerably faster than the reinitiated *ϕ6EC*.

An accurate determination of k_{elong} and k_{poly}

To support this initial observation, we obtained a more quantitative determination of k_{elong} and k_{poly} in the case of reinitiated and randomly initiated *ϕ6ECs*, respectively. We converted the electrophoretic mobilities of the elongation intermediates of reinitiated *ϕ6EC* to a number of replicated nucleotides by using a calibration curve relating the two quantities (Supplementary Data and Figure S2). We converted only the earlier time points in Figure 2B, because the decreasing differences in the electrophoretic mobilities in the later reaction stages precluded an accurate determination of the number of replicated nucleotides. The results show that the number of replicated nucleotides after reinitiation increased linearly with time, indicating that the reinitiated *ϕ6EC* exhibited a constant k_{elong} (Figure 3A, red points). k_{elong} was deduced from the slope of the linear fit (Figure 3A, solid red line) and averaged 2 ± 1 nt s^{-1} (mean and standard deviation determined from six experiments).

Independently, we determined an improved estimate for k_{poly} for randomly-initiated *ϕ6RdRP* replication, by extrapolating the data to the minimum time τ necessary for the conversion of a single 4 kb ssRNA to its 4 kb dsRNA product, as previously reported (14). For example, to extract the value of τ from the data in Figure 2D, the normalized intensity of the band corresponding to 4 kb dsRNA was plotted as a function of polymerization time, and the experimental points were fitted to a straight line (Figure 3B, solid red line). The x-intercept of the linear fit yielded $\tau = 287 \pm 42$ s, which corresponds to $k_{poly} = 15 \pm 3$ nt s^{-1} (mean and standard deviation deduced from three experiments). These more accurate values of k_{elong} and k_{poly} thus establish that the elongation

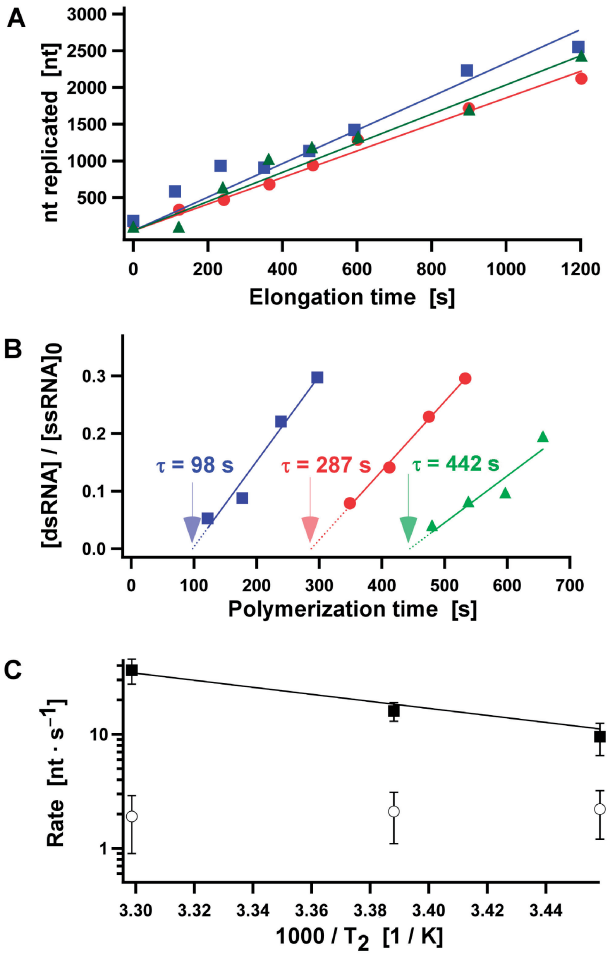

Figure 3. Stalling of *ϕ6EC* reduces the elongation rate (k_{elong}) following reinitiation. **(A)** Progression of the reinitiated *ϕ6EC* along the 4 kb ssRNA at three different values of T_2 (T_2 = 16°C, green triangles; T_2 = 22°C, red circles; T_2 = 30°C, blue squares). Stalling of the *ϕ6EC* was carried out at T_1 = 22°C. The number of replicated nucleotides (nt) was determined from the electrophoretic mobilities of elongation intermediates using the calibration curve in Figure S2C as described in the Supplementary Data. Solid lines are linear fits to the data. k_{elong} are determined from the slopes of the corresponding linear fits. **(B)** The relative concentration of the replication products as a function of the polymerization time during randomly-initiated *ϕ6 RdRP* replication at three different values of T_2 (T_2 = 16°C, green triangles; T_2 = 22°C, red circles; T_2 = 30°C, blue squares). The incubation of 4 kb ssRNA and *ϕ6 RdRP* prior to the addition of the NTPs was carried at T_1 = 22°C. Values of τ, representing the minimal sum of the initiation and elongation times during randomly-initiated *ϕ6 RdRP* replication, were determined by the *x*-intercept extrapolated from the linear fits and used to calculate the polymerization rates (k_{poly}) as described in the text. **(C)** Arrhenius plot of the elongation and polymerization rates for the reinitiated *ϕ6EC* (open circles), and for randomly-initiated *ϕ6 RdRP* replication (filled squares), respectively. The data obtained with random initiation was fitted to the Arrhenius equation (solid line).

rate of randomly-initiated *ϕ6EC* exceeds that of reinitiated *ϕ6EC* by nearly an order of magnitude.

k_{elong} of the reinitiated *ϕ6EC* is independent of temperature

To gain insight into the mechanisms underlying the observed rate reduction, we compared the temperature dependence of k_{elong} and k_{poly}. To measure the temperature dependence of k_{elong}, we first stalled *ϕ6EC* at temperature T_1 for 15 min, equilibrated for 5 min at temperature T_2, and reinitiated the *ϕ6EC* (Figure 2A). We first fixed T_1 at 22°C and varied T_2 (16°C, 22°C, or 30°C) (Supplementary Figure S5). Using calibration described above, we found that the number of replicated nucleotides by the reinitiated *ϕ6EC*s increased linearly with time for all three T_2 (Figure 3A, green, red and blue solid lines correspond to T_2 = 16°C, T_2 = 22°C, and T_2 = 30°C, respectively). Surprisingly, we found k_{elong} to be independent of T_2 (k_{elong} of $2 \pm 1\,nt\,s^{-1}$ for all three T_2). The experiment was then repeated at different T_1 (16°C and 30°C) (Supplementary Figure S5). Here, too, we found that k_{elong} remained constant during replication and was unaffected by changes in T_1. Furthermore, the data reveals that k_{elong} is independent of T_1. In summary, we can conclude that over the range tested, k_{elong} of the reinitiated *ϕ6EC* is independent of temperature.

For comparison, we applied the same temperature variation to the unstalled enzyme. As above, three different values of T_1 and T_2 were tested (16°C, 22°C, and 30°C for both T_1 and T_2) (Supplementary Figure S6). k_{poly} was determined by measuring τ as in Figure 2D. At fixed T_1 = 22°C, we found that k_{poly} increased with increasing T_2, from $9 \pm 4\,nt\,s^{-1}$ at T_2 = 16°C, to $15 \pm 3\,nt\,s^{-1}$ at T_2 = 22°C, and finally to $43 \pm 14\,nt\,s^{-1}$ at T_2 = 30°C (mean and standard deviation deduced from three experiments). No detectable changes in the measured k_{poly} were observed when T_1 was changed to 16°C or 30°C (Supplementary Figure S6). A comparison of k_{elong} and k_{poly} is revealing: first, k_{poly} is consistently greater than k_{elong} over the entire temperature range probed (Figure 3C): the rate reduction is not a particularity of experiments performed at room temperature; in addition, in contrast to the temperature-insensitive k_{elong}, the polymerization rate k_{poly} of randomly-initiated *ϕ6EC* showed significant dependence on T_2 (Figure 3C), from which we deduced an activation free energy for the rate-determining step of 24 k_BT by fitting the data to an Arrhenius equation (solid line in Figure 3C).

k_{elong} is insensitive to the nucleotide concentration during stalling and to the length of elongated RNA prior to stalling

To relate the observed differences between the kinetic profiles of reinitiated and randomly-initiated *ϕ6ECs* to specific regions of *ϕ6RdRP* structure, we investigated a number of factors that could affect the interactions within the *ϕ6EC*. These experiments were performed at a fixed T_1 and T_2 of 22°C.

To determine whether the NTP concentration during stalling affected the rate of the reinitiated *ϕ6ECs*, we varied it from 0–2.5 mM per NTP. The stalled *ϕ6ECs* were reinitiated by the addition of a mixture of all four NTPs to bring the final concentration of each NTP after reinitiation to 2.5 mM, as above. Aliquots were collected at 4 min and 8 min after reinitiation and loaded on agarose gel (Supplementary Figure S7A). In the complete absence of NTPs during stalling, only the products of randomly-initiated *ϕ6ECs* were detected, as expected (Figure 4A). As the NTP concentration during the stalling stage was

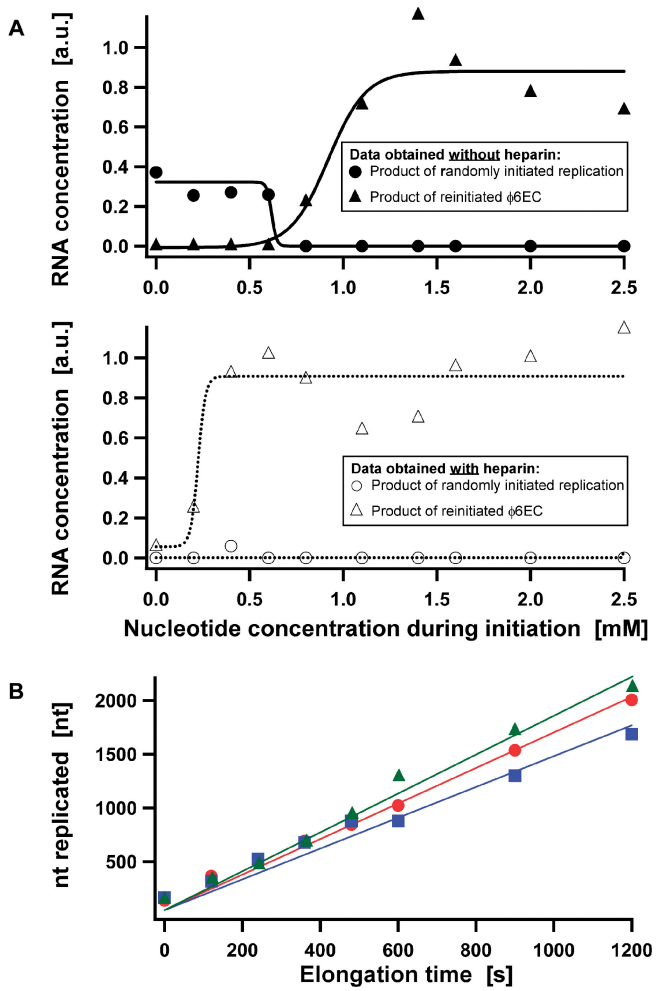

Figure 4. Effects of the NTP concentration during the stalling stage and the length of dsRNA synthesized prior stalling on k_{elong} of the reinitiated *ϕ6EC*. **(A)** *ϕ6 RdRP* stalling was carried out at different NTP concentrations, but the reinitiated *ϕ6EC* performed the reaction at a constant NTP concentration of 2.5 mM per NTP. The reinitiated *ϕ6EC* kinetics at each NTP concentration were studied in the absence and presence of heparin. Heparin was added after the stalling step, prior to reinitiation. Relative concentrations of the replication products and intermediates at 8 min after the addition of UTP were obtained by dividing the intensity of the corresponding band with the intensity of the 3 kb dsDNA band of the dsDNA ladder. In both plots, circles refer to the product of the randomly-initiated replication (4 kb dsRNA), whereas triangles correspond to the replication intermediates of the reinitiated *ϕ6EC* (Supplementary Figure S7). The experimental points were fitted to a sigmoidal curve. **(B)** The number of nucleotide replicated prior stalling was 3, 7, or 50 nts and the data is indicated with circles, squares, and triangles, respectively. Solid lines are linear fits to the data.

increased from 0.2 mM to 0.6 mM, this remained the case: only the products of randomly-initiated replication were present, and no detectable slow population of reinitiated *ϕ6EC* was observed (Figure 4A top, circles). However, once the NTP concentration exceeded 0.8 mM, the products of randomly-initiated replication were no longer observed; instead the slowly-migrating, distinct bands of elongation intermediates attributable to reinitiated *ϕ6ECs* appeared (Figure 4A top, triangles). Concentrations of reinitiated *ϕ6ECs* increased as the NTP concentration during stalling was further increased to 1.4 mM, but beyond 1.4 mM no further increase was detected. We note that little variation was observed between the electrophoretic mobilities of the reinitiated *ϕ6EC*, indicating similar k_{elong} (Supplementary Figure S7A).

Finally, to absolutely confirm that the bands detected below 0.8 mM NTP concentration during stalling were indeed the products of randomly-initiated replication, the experiments were repeated in the presence of heparin following stalling (Supplementary Figure S7B). Heparin is known to inactivate free (i.e. unstalled) RNA polymerase (13), and can thus prevent random initiation after stalling. We indeed observed the products of randomly-initiated replication either entirely disappeared or were greatly reduced in the presence of heparin (Figure 4A bottom, circles). In contrast, the presence of heparin did not reduce the concentration of the reinitiated *ϕ6ECs*; however, it decreased the nucleotide concentration during stalling at which successfully reinitiated *ϕ6ECs* were detected (Figure 4A bottom, triangles). We can thus conclude that NTP concentration during the stalling stage affects the likelihood of forming stalled *ϕ6ECs*, leaving the subsequent dynamics as captured by k_{elong} entirely unaffected.

The site at which the *ϕ6EC* stalls on the template strand determines the length of the dsRNA protruding from the *ϕ6 RdRP* product tunnel (Figure 1B). To investigate the effect of the dsRNA length on the k_{elong} of reinitiated *ϕ6EC*, we synthesized replication templates with a stalling site at the third or seventh nucleotide. These replication templates were designed to stall *ϕ6EC* in the presence of three NTPs (i.e. ATP, CTP, and GTP) and reinitiate by the addition of UTP, as in the case of 4 kb ssRNA. On all these templates, the number of replicated nucleotide increased linearly with the elongation time (Figure 4B), as observed previously. Similarly, the observed k_{elong} were measured to be $2 \pm 1\ \text{nt s}^{-1}$ in all instances (mean and standard deviation deduced from three experiments). Thus, we find the dynamics of the reinitiated *ϕ6EC* to be insensitive to the length of the elongated RNA prior stalling.

Kinetics of the reinitiated elongation complex during *ϕ6 RdRP* transcription

Different secondary structures of replication and transcription templates may interact differently with *ϕ6 RdRP* within the stalled *ϕ6ECs* (Figure 1), as RNA secondary structure elements located in viral RNAs have been shown to regulate *RdRP* polymerization (22,23). To test the role of template secondary structure on *ϕ6EC* kinetics after reinitiation, a 4 kb long transcription template was designed with a 50 nt long single-stranded sequence devoid of adenine at the 3′-end of the transcribed strand (Figure 5A). The design of the transcription template included a nick solely to facilitate separation of the template from the product on gel. After *ϕ6EC* stalling and introduction of the missing UTP, *ϕ6EC* can reinitiate yielding a branched elongation intermediates. At the end of transcription, a completely double-stranded 3 kb dsRNA (Product A) and partially double-stranded RNA (Product B) remained.

Similarly to the above study of *ϕ6RdRP* replication, we measured k_{elong} of the reinitiated *ϕ6EC* and k_{poly} of

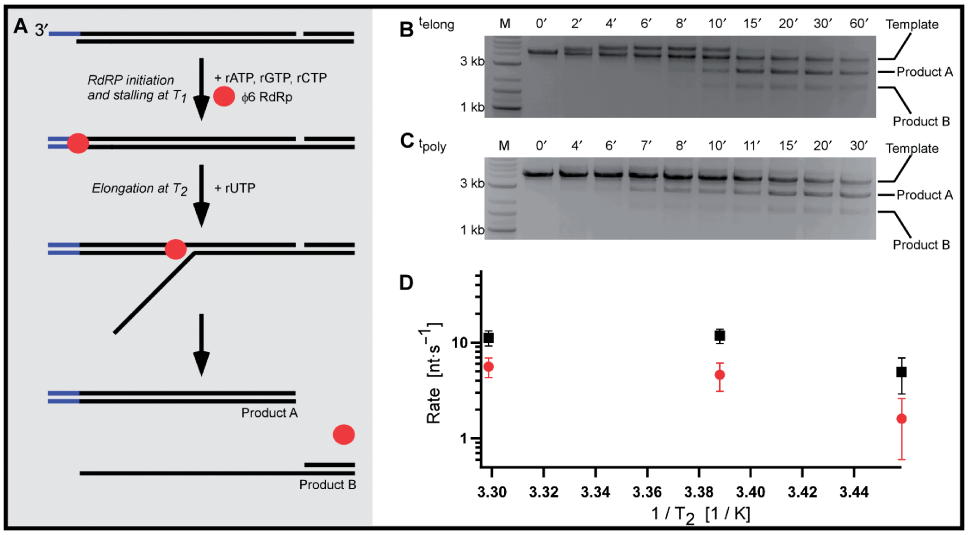

Figure 5. Stalling affects the k_{elong} during transcription less than during replication. **(A)** Schematic representation of *ϕ6 RdRP* transcription with stalling. The transcription template was synthesized by hybridizing three ssRNAs. The single-stranded sequence transcribed prior stalling is positioned at the 3′-end of the template strand. *ϕ6 RdRP* is stalled with three NTPs at temperature T_1, and transcription reinitiated by the addition of UTP at temperature T_2. When the reaction is complete, Products A and B result. **(B)** Agarose gel analysis of aliquots collected at different time points after the reinitiation of the stalled *ϕ6EC*. The transcription template, Product A and Product B bands are indicated. Transcription intermediates have the lowest electrophoretic mobility and can be observed at 2′, 4′, 6′, 8′ and 10′ after reinitiation. **(C)** Transcription by *ϕ6 RdRP* in the absence of stalling. Aliquots collected at different polymerization times were analyzed on agarose gel. **(D)** An Arrhenius plot of the experimentally-observed elongation (red circles) and polymerization rates (black squares) of the reinitiated *ϕ6EC* and randomly initiated *ϕ6 RdRP* transcription, respectively, during the transcription reaction.

randomly initiated *ϕ6EC* during transcription. First, k_{elong} on the transcription template after reinitiation was assayed at three different T_2 (16°C, 22°C or 30°C). The elongation intermediates could be readily observed and displayed a decreased electrophoretic mobility compared to the free transcription template or the stalled *ϕ6EC* as a result of their higher molecular weight and branched structure (Supplementary Figure 5B). The electrophoretic mobility of Product A corresponds well to that of 2876 bp long dsRNA, and the electrophoretic mobility of Product B agrees with the value predicted by the previously constructed calibration curves of RNA hybrids (Supplementary Figure S2C). As in the replication reaction, an appreciable fraction of the transcription template binds *ϕ6 RdRP*, stalls the *ϕ6EC*, and enables the synchronized reinitiation of the stalled *ϕ6EC* after UTP addition, as judged from the well-defined bands corresponding to the elongation intermediates (Figure 5B, lane 2). In these transcription experiments, the more complex structure of the elongation intermediates prevented determination of k_{elong} from the electrophoretic mobilities of the reaction intermediates. Rather, k_{elong} was determined by dividing the length of the transcribed template by the typical time required to complete transcription. This time was approximated by measuring the mid-point between time t_1, when the Product A band was first detected, and time t_2, when the intensity of the elongation intermediate was observed to decrease. We report that k_{elong} during transcription was comparable to k_{elong} during replication at the lowest T_2 ($1.6 \pm 1.0\,nt\,s^{-1}$ at $T_2 = 16°C$) but increased somewhat at higher T_2 ($4.6 \pm 1.5\,nt\,s^{-1}$ at $T_2 = 22°C$) and $5.6 \pm 1.3\,nt\,s^{-1}$ at $T_2 = 30°C$ (red circles in Figure 5D) (mean and standard deviation deduced from three experiments).

We then investigated the kinetics of transcription by randomly-initiated *ϕ6EC*. In the transcription reaction with the unstalled *ϕ6EC*, the transcription products could readily be observed (Figure 5C). However, no elongation intermediates were detected, due to a lack of synchrony in the population of *ϕ6EC*s. We plotted the intensity of the Product A band as a function of the polymerization time and fitted the experimental points to a line. The τ values obtained were used to determine k_{poly} as above. At $T_1 = 22°C$, the k_{poly} obtained for the randomly-initiated transcription was $5 \pm 2\,nt\,s^{-1}$ at $T_2 = 16°C$, $k_{poly} = 12 \pm 2\,nt\,s^{-1}$ at $T_2 = 22°C$, and $k_{poly} = 11 \pm 2\,nt\,s^{-1}$ at $T_2 = 30°C$ (black squares in Figure 5D). We thus observe that the values of k_{elong} are again consistently slower than the values of k_{poly} of the randomly-initiated *ϕ6 RdRP*. However, the observed differences are less pronounced than in the case of the replication reaction. In addition, in transcription, the k_{elong} and k_{poly} display similar temperature sensitivities, in contrast to the replication reaction, where considerable differences in the temperature trends were observed.

DISCUSSION

We have established that a reinitiated *ϕ6EC* displays a decreased k_{elong} compared to a randomly-initiated *ϕ6EC*. The reduced k_{elong} of the reinitiated *ϕ6EC* remained constant during the replication of at least the first 2.5 kb of the 4 kb ssRNA replication template (Figure 3A). Furthermore, our estimate of the time point at which replication of 4 kb ssRNA was complete (Figure 2B) yielded an overall elongation rate between $1.2\,nt\,s^{-1}$ and

$2.3\,nt\,s^{-1}$, in a good agreement with the rate determined for the replication of the first 2.5 kb via fitting the electrophoretic mobilities of the replication intermediate ($2 \pm 1 nt\,s^{-1}$). Thus, the reinitiated *ϕ6EC* elongates with a reduced rate throughout the template, from which we conclude that the conversion undergone by *ϕ6EC* during the stalling step is irreversible.

This irreversible conversion to the inhibited *ϕ6EC* state must be promoted during stalling, as the initial stages prior to *ϕ6EC* stalling proceeded similarly in both stalled and unstalled reactions. An upper limit for the time needed for the conversion to the inhibited *ϕ6EC* state could be deduced from the shortest time required to observe a synchronized population of reinitiated *ϕ6EC*s (2 min at $T_1 = 22^{\circ}C$; Supplementary Figure S8). Analysis of the temperature dependence of the reinitiated and randomly-initiated *ϕ6EC* showed considerably different behaviour for the two complexes (Figure 3C). The kinetics of a randomly-initiated *ϕ6EC* could be described well within an Arrhenius model and yielded activation energy of 24 k_BT for polymerization. In contrast, the kinetics of a reinitiated *ϕ6EC* showed little temperature dependence of the elongation rates, implying that the conversion event during the stalling step may be insensitive to temperature. The irreversible conversion was similarly insensitive to both the NTP concentration during stalling and the length of the replicated template before stalling (Figure 4).

It is interesting to consider the possible nature of this irreversible conversion. A comparison of replication and transcription revealed that inhibition of the reinitiated *ϕ6EC* was appreciably greater with single- than double-stranded templates (Figures 3 and 5). This suggests that the template type has an effect on the conversion to the inhibited *ϕ6EC* state. This may be akin to the regulation of activity observed for other nucleic acid polymerases via either specific (e.g. RNA hairpin-protein) or nonspecific (e.g. electrostatic, hydrophobic) interactions (24–26). The interactions between *ϕ6 RdRP* and its template that are responsible for the conversion to the inhibited state do not appear to be related to a particular RNA secondary structure, as the template strands were denatured prior to stalling and were thus most likely present as an ensemble of different RNA folds stable under the applied reaction conditions. The fact that replication is affected more than transcription may suggest the nature of the nonspecific interactions involved (e.g. hydrophobic interactions promoted by the exposed bases of ssRNA). However, the fact that replication is affected more than transcription may also implicate other nonspecific interactions that occur with a higher probability in the case of ssRNA template simply as a consequence of its lower persistence length, which gives rise to a lower radius of gyration (27) and thus a higher local concentration of the template at the enzyme surface. Nonspecific RNA-*ϕ6 RdRP* interactions may cause the template RNA to interfere with the different tunnels in the enzyme and impair their proper functioning (e.g. they might limit exchange of free NTPs in the NTP channel, exit of the dsRNA in the product tunnel, or entry of the template strand in the template tunnel), resulting in a decrease in the overall elongation rates. Alternatively, RNA-*ϕ6 RdRP* interactions could trigger conformational changes within the *ϕ6RdRP* that result in suboptimal reaction rates.

It is evident that complex enzymes such as *ϕ6 RdRPs* are regulated through multiple mechanisms, and their sum total dictates both the enzyme rates. It is thus intriguing that even a simple stalling event can lead to considerable changes in enzyme dynamics. It remains to be seen whether the reduction in elongation rate after stalling is a general property of viral *RdRP*s. The arrest of the elongation complex could be biologically relevant during the viral life cycle, in which RNA replication and transcription are highly regulated (28). In addition, it could affect the frequency of RNA recombination and thus the adaptation of RNA viruses to their environment (10,11). More technically, many experiments have applied stalling protocols to measure elongation rates of polymerases (13,16–18). As shown here for *ϕ6 RdRP*, these measurements may provide inaccurate values, in the absence of confirmation that the enzyme is unaffected by stalling. For example, when *T7* RNA polymerase (*T7 RNAP*) was stalled and subsequently reinitiated, the resulting elongation rate was as low as $2\,nt\,s^{-1}$ as judged from a study by Ferrari and co-workers (17). By contrast, unstalled *T7 RNAP* exhibited elongation rates that range from 40–400 $nt\,s^{-1}$ (29–31). Finally, polymerases may not be the only enzymes whose activity can be regulated via stalling. For instance, Kowalczykowski and co-workers recently showed that RecBCD helicase switches lead motors in response to the stalling at a specific DNA sequence, similarly resulting in a rate reduction of motor translocation (32).

SUPPLEMENTARY DATA

Supplementary Data are available at NAR Online.

ACKNOWLEDGEMENTS

We thank W. Kamping and R. Tarkiainen for their experimental work and R. Tuma for fruitful discussions.

FUNDING

Nanoned, The Netherlands Organization for Scientific Research, and the European Science Foundation (grants to N.H.D.); the Finish Center of Excellence Program 2006-2011 (1213467 to D.H.B.), the Academy of Finland and Nanotechnology (700036 to D.H.B.); Helsinki Graduate School of Biotechnology and Molecular Biology (funding of A.P.A.). Funding for open access charge: The Netherlands Organization for Scientific Research.

Conflict of interest statement. None declared.

REFERENCES

1. Cerutti,H. and Casas-Mollano,J. A. (2006) On the origin and functions of RNA-mediated silencing: From protists to man. *Curr. Genet.*, **50**, 81–99.

2. Ferrer-Orta,C., Arias,A., Escarmis,C. and Verdaguer,N. (2006) A comparison of viral RNA-dependent RNA polymerases. *Curr. Opin. Struct. Biol.*, **16**, 27–34.
3. Ortin,J. and Parra,F. (2006) Structure and function of RNA replication. *Annu. Rev. Microbiol.*, **60**, 305–326.
4. Arnold,J.J., Gohara,D.W. and Cameron,C.E. (2004) Poliovirus RNA-dependent RNA polymerase (3Dpol): Pre-steady-state kinetic analysis of ribonucleotide incorporation in the presence of Mn^{2+}. *Biochemistry*, **43**, 5138–5148.
5. Cramer,J., Jaeger,J. and Restle,T. (2006) Biochemical and pre-steady-state kinetic characterization of the hepatitis C virus RNA polymerase (NS5BΔ21, HC-J4). *Biochemistry*, **45**, 3610–3619.
6. Thal,M.A., Wasik,B.R., Posto,J. and Hardy,R.W. (2007) Template requirements for recognition and copying by Sindbis virus RNA-dependent RNA polymerase. *Virology*, **358**, 221–232.
7. Yang,H.Y., Gottlieb,P., Wei,H., Bamford,D.H. and Makeyev,E.V. (2003) Temperature requirements for initiation of RNA-dependent RNA polymerization. *Virology*, **314**, 706–715.
8. van Dijk,A.A., Makeyev,E.V. and Bamford,D.H. (2004) Initiation of viral RNA-dependent RNA polymerization. *J. Gen. Virol.*, **85**, 1077–1093.
9. Neufeld,K.L., Richards,O.C. and Ehrenfeld,E. (1991) Purification, characterization, and comparison of poliovirus RNA polymerase from native and recombinant sources. *J. Biol. Chem.*, **266**, 24–24.
10. Mindich,L. (2004) Packaging, replication and recombination of the segmented genomes of bacteriophage ϕ6 and its relatives. *Virus Res.*, **101**, 83–92.
11. Worobey,M. and Holmes,E.C. (1999) Evolutionary aspects of recombination in RNA viruses. *J. Gen. Virol.*, **80**, 2535–2543.
12. Koch,U. and Narjes,F. (2007) Recent progress in the development of inhibitors of the hepatitis C virus RNA-dependent RNA polymerase. *Curr. Top. Med. Chem.*, **7**, 1302–1329.
13. Sun,J.H. and Kao,C.C. (1997) RNA synthesis by the BMV RNA-dependent RNA polymerase: transition from initiation to elongation. *Virology*, **233**, 63–73.
14. Makeyev,E.V. and Bamford,D.H. (2000) Replicase activity of purified recombinant protein P2 of double-stranded RNA bacteriophage ϕ6. *EMBO J.*, **19**, 124–133.
15. Butcher,S.J., Grimes,J.M., Makeyev,E.V., Bamford,D.H. and Stuart,D.L. (2001) A mechanism for initiating RNA-dependent RNA polymerization. *Nature*, **410**, 235–240.
16. Davenport,R.J., Wuite,G. J. L., Landick,R. and Bustamante,C. (2000) Single-molecule study of transcriptional pausing and arrest by *E. coli* RNA polymerase. *Science*, **287**, 2497–2500.
17. Ferrari,R., Rivetti,C. and Dieci,G. (2004) Transcription reinitiation properties of bacteriophage T7 RNA polymerase. *Biochem. Biophys. Res. Commun.*, **315**, 376–380.
18. Tolic-Norrelykke,S.F., Engh,A.M., Landick,R. and Gelles,J. (2004) Diversity in the rates of transcript elongation by single RNA polymerase molecules. *J. Biol. Chem.*, **279**, 3292–3299.
19. Studier,F.W. and Moffatt,B.A. (1986) Use of bacteriophage T7 RNA polymerase to direct selective high-level expression of cloned genes. *J. Mol. Biol.*, **189**, 113–130.
20. Petrushenko,Z.M., Lai,C.H., Rai,R. and Rybenkov,V.V. (2006) DNA reshaping by MukB – Right-handed knotting, left-handed supercoiling. *J. Biol. Chem.*, **281**, 4606–4615.
21. Vilfan,I.D., Kamping,W., van den Hout,M., Candelli,A., Hage,S. and Dekker,N.H. (2007) An RNA toolbox for single-molecule force spectroscopy studies. *Nucleic Acids Res.*, **35**, 6625–6639.
22. Deiman,B., Kortlever,R.M. and Pleij,C.W.A. (1997) The role of the pseudoknot at the 3′ end of turnip yellow mosaic virus RNA in minus-strand synthesis by the viral RNA-dependent RNA polymerase. *J. Virol.*, **71**, 5990–5996.
23. Osman,T.A. M., Hemenway,C.L. and Buck,K.W. (2000) Role of the 3′ tRNA-like structure in TMV minus-strand RNA synthesis by the viral RNA-dependent RNA polymerase in vitro. *J. Virol.*, **74**, 11–11.
24. Artsimovitch,I. and Landick,R. (1998) Interaction of a nascent RNA structure with RNA polymerase is required for hairpin-dependent transcriptional pausing but not for transcript release. *Genes Dev.*, **12**, 3110–3122.
25. Rivetti,C., Guthold,M. and Bustamante,C. (1999) Wrapping of DNA around the *E.coli* RNA polymerase open promoter complex. *EMBO J.*, **18**, 4464–4475.
26. Toulokhonov,I. and Landick,R. (2003) The flap domain is required for pause RNA hairpin inhibition of catalysis by RNA polymerase and can modulate intrinsic termination. *Mol. Cell*, **12**, 1125–1136.
27. Sedlak,M. (2001) In Radeva,T. (ed.), *Physical chemistry of polyelectrolytes*. CRC Press, New York, pp. 1–58.
28. Plumet,S., Duprex,W.P. and Gerlier,D. (2005) Dynamics of viral RNA synthesis during Measles virus infection. *J. Biol. Chem.*, **79**, 6900–6908.
29. Kim,J.H. and Larson,R.G. (2007) Single-molecule analysis of 1D diffusion and transcription elongation of T7 RNA polymerase along individual stretched DNA molecules. *Nucleic Acids Res.*, **35**, 3848–3858.
30. Skinner,G.M., Baumann,C.G., Quinn,D.M., Molloy,J.E. and Hoggett,J.G. (2004) Promoter binding, initiation, and elongation by bacteriophage T7 RNA polymerase - A single-molecule view of the transcription cycle. *J. Biol. Chem.*, **279**, 3239–3244.
31. Uptain,S.M., Kane,C.M. and Chamberlin,M.J. (1997) Basic mechanisms of transcript elongation and its regulation. *Annu. Rev. Biochem.*, **66**, 117–172.
32. Spies,M., Amitani,I., Baskin,R.J. and Kowalczykowski,S.C. (2007) RecBCD enzyme switches lead motor subunits in response to χ recognition. *Cell*, **131**, 694–705.